PHYSICAL REVIEW E **66**, 015102(R) (2002)

Crumpled wires in two dimensions

C. C. Donato, M. A. F. Gomes, and R. E. de Souza
Departamento de Física, Universidade Federal de Pernambuco, 50670-901, Recife PE, Brazil
(Received 24 January 2002; published 18 July 2002)

Geometric and statistical properties of wires injected into a two-dimensional cavity with three different injection geometries are investigated. Complex patterns of folds are observed and studied as a function of the length of the wire. The mass-size relation and the distribution function $n(s)$ of loops with internal area s formed as a consequence of the folded structure of the wire are examined. Several scaling laws are found and a hierarchical model is introduced to explain the experimental behavior observed in this two-dimensional crumpling process.

DOI: 10.1103/PhysRevE.66.015102 PACS number(s): 05.90.+m, 05.70.Np, 47.53.+n, 68.35.Rh

Crumpling is both a very interesting problem in its own right and a ubiquitous physical phenomenon [1]. In spite of the scientific and technological importance of phenomena associated with microscopic and macroscopic crumpled materials, our understanding of the behavior of these systems is still limited. In fact, extreme nonlinear effects and irreversibility observed in crumpling of structures with the topology of the plane introduce great difficulties in the theory of elasticity and in the geometry of surfaces [1]. In the past few years, however, theoretical and experimental aspects of physics of crumpled sheets have been a subject of growing interest in many areas of study, e.g., acoustic emission [2], continuous mechanics [3], growth models [4], packing problems [5], polymer, membrane, and interface physics [6], and universality [7], among others. On the other hand, crumpled structures with different topologies, as exemplified by a squeezed ball of wire, have been much less studied in the physics literature. Some geometric, statistical, and physical aspects of irreversibly crumpled wires in three-dimensional (3D) space were examined ten years ago and, in particular, robust scaling laws and fractal dimensions associated with these disordered systems were reported [8].

Here, on the contrary, we present results of an experimental analysis of crumpled structures in 2D obtained by irreversible squeezing of macroscopic pieces of copper wires within a *two-dimensional* planar transparent cavity. Irreversibility here means that if the constraints due to the cavity are removed, the crumpled wire does not restore the initial situation. We will show that the structure of this 2D crumpling process is *remarkably* different from crumpling processes of sheets in 3D. We have also succeeded in explaining the experimental data with a hierarchical crumpling model based on a cascade of loops of decreasing sizes.

The apparatus used to obtain the digital images of the 2D configurations of crumpled wires (CW) is shown in Fig. 1. It consists of a transparent cell formed by the superposition of two disks of Plexiglas with a total height of 1.8 cm, an external diameter of 30.0 cm, and a circular cavity of 20.0 cm diameter and 0.11 cm height, which can accommodate configurations of a *single* layer of CW of diameter (gauge) $\zeta = 0.10$ cm. In order to reduce friction, the cavity of the cell was polished and the 19AWG copper wire used in the experiment had a varnished surface. The cavity and the wire operated in a dry regime, free of lubrication. Radial channels were made to provide three different ways of injecting the wire into the cell at the angles of 10°, 90°, and 180° (Fig. 1). The photographs were taken with an Olympus C-3040ZOOM digital camera with a resolution of 3 megapixels that was connected to a computer and assembled 30 cm over the cell. To avoid picture artifacts by light reflections, a cylindrical screen was placed around the cell. An injection experiment begins fitting a straight wire in the opposite channels and subsequently pushing manually and uniformly the wire on both sides of the cell toward the interior of the cavity. The injection velocity at each channel in these experiments was typically of the order of 1 cm/s.

When a thin wire of length L is injected inside the cell, the wire bends if its length is slightly larger than the diameter of the cavity, $2R_0$. There is a critical length $L_c = h_1$, given by the experimental ratio $\eta_c = h_1/2\pi R_0 = 0.684 \pm 0.008$, when the wire touches itself forming the first loop [Fig. 2(a)]. For larger L, the wire begins to crumple progressively into a complex nonuniform shape as illustrated in Figs. 2(b)–2(d). The photographs in Fig. 2 refer to the regime of injection along the 180° channels. For wires with the largest lengths, the crumpled structures become progressively more rigid, the difficulty in the injection increases, and the injection velocity

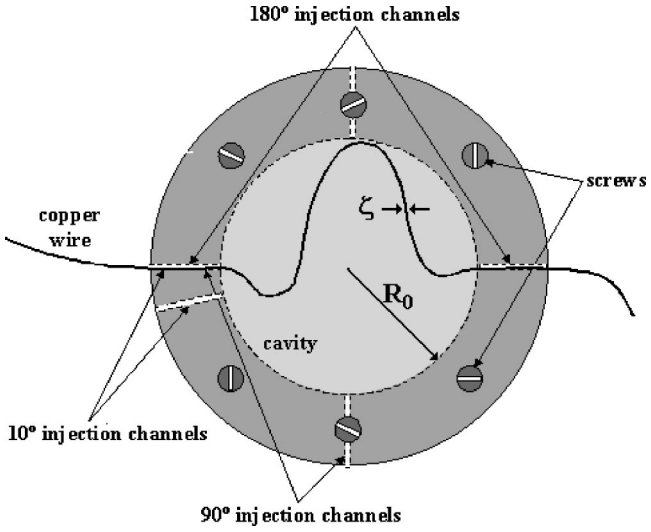

FIG. 1. Diagram of the 2D injection cell used in the experiments.

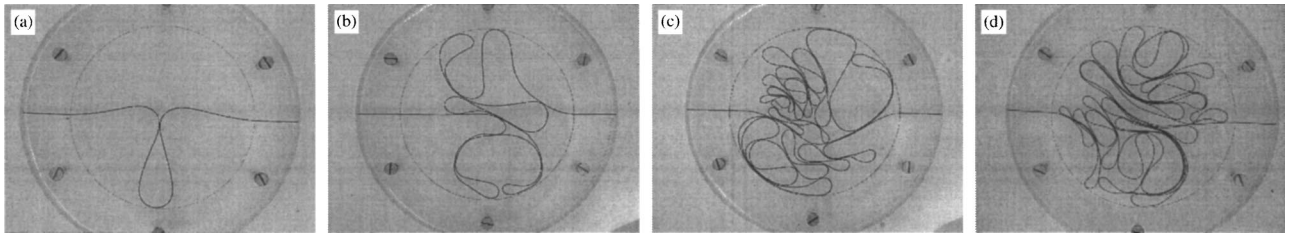

FIG. 2. Typical conformations of crumpled wires in 2D with length (a) 42.9, (b) 150, (c) 300, and (d) 470 cm.

is somewhat smaller. However, the observed phenomena are widely independent of the injection speed for all intervals of injection velocities compatible with a manual process. There is a moment when the injection velocity goes rapidly to zero. In this particular moment, the CW reaches a tight-packing (TP) configuration as that shown in Fig. 2(d). The TP configuration occurs for the maximum occupation probability $p_{\max} \equiv \zeta L_{\max}/\pi R_0^2$, where $L_{\max}$ is the maximum length of wire that can be introduced within the cavity. An experimental estimate of this maximum occupation probability is $p_{\max} = 0.140 \pm 0.006$. The mechanical behavior of the samples appears to be quite different near and below $p_{\max}$. The 2D crumpled structure is rigid for $p = p_{\max}$; it is completely jammed within the cavity and it is impossible to continue the injection of wire into the cell. To rule out any possibility of the TP configuration being a consequence of friction effects, we carried out experiments where the cavity was filled with mineral oil. The results perfectly agreed with the dry regime ones. Geometric patterns of CW for injection angles of 10° and 90° are different from those exhibited in Fig. 2 only for the smaller lengths. When L increases, the configurations of CW converge rapidly to a typical structure that does not depend on the injection angle. Because of a lack of space, only the data associated with the experiments with the 180° channels are shown [9]. The crumpled patterns of wire observed within the cell are basically due to the formation of a cascade of loops of decreasing size (Fig. 2). During the progressive injection of wire into the cell, the cascade of loops evolves in such way that it is common to observe localized and global rearrangements of loops previously formed.

One of the most basic physical properties when dealing with complex patterns and fractal structures is the dependence $M(R)$ of the mass of the system within a circle of radius R [10]. This quantity is exemplified in the log-log plot of Fig. 3 in arbitrary units, for an ensemble of 7 CW in the TP limit, with average $L = 438$ cm, corresponding to lengths varying from 410 to 470 cm. We observe that the mass (or projected area ζL) of the crumpled structures presents a tendency to scale as a power law in R, from $R = 0.1$ cm to $R = R_0 = 10$ cm. From this figure we obtain $M(R) \sim R^D$, with $D = 1.9 \pm 0.1$, for 0.6 cm $\leqslant R \leqslant 6$ cm; that is, the TP is two-dimensional within the statistical fluctuations. At this point, some information on the method used to obtain $M(R)$ in Fig. 3 is needed. The measurement of M as a function of R was made in two steps: for 4 cm $< R <$ 10 cm, $M(R)$ was measured within a single ball with the origin at the geometrical center of the cell; and for 0.1 cm $< R <$ 4.0 cm, $M(R)$ was taken as the average mass within five to six equivalent disjoint balls whose centers were localized in different points of the wire taken at random but subject to the further constraint of nonoverlap with the border of the cell. This procedure is important to counterbalance a common distortion leading to a depletion of the mass near the center of the cell if a single ball is used.

As the length of wire injected into the cavity increases, i.e., as the occupation probability $p = \zeta L/\pi R_0^2$ rises, the total number of loops, n_l, formed as a consequence of wire-wire contacts, also grows. The experimental dependence of n_l with p and the corresponding fluctuations are shown in Fig. 4. The log-log plot of $n_l(p)$ shows two different behaviors: a shoulder for $p \lesssim 0.032$ and a power-law asymptotic dependence $n_l \sim p^{1.8 \pm 0.2}$ for $0.032 \lesssim p \lesssim 0.140$. The rate of loop formation presents the largest value in the beginning of the first region, when the incipient CW behaves as a soft structure. Moreover, the total number of contacts between loops (Fig. 4, inset) scales as $n_{ll} \sim p^{2.2 \pm 0.2}$ in the same interval. The last result is reminiscent of Flory's mean-field argument [11], which suggests that n_{ll} should scale with the repulsive energy within the CW, that is, with p^2. The number of coordination or contacts per loop, $\gamma = n_{ll}/n_l$ (not shown), increases asymptotically as $\gamma \sim p^{0.7 \pm 0.2}$ in the interval $0.032 \lesssim p \lesssim 0.140$.

The TP limit in our experiments is associated with 2D configurations of CW with a total number of loops varying in the interval $n_l = 22$ to $n_l = 45$. In all we had 249 loops for seven equivalent experiments of CW with the largest lengths (i.e., ≈ 35.5 loops per experiment with $L = L_{max}$). If loops

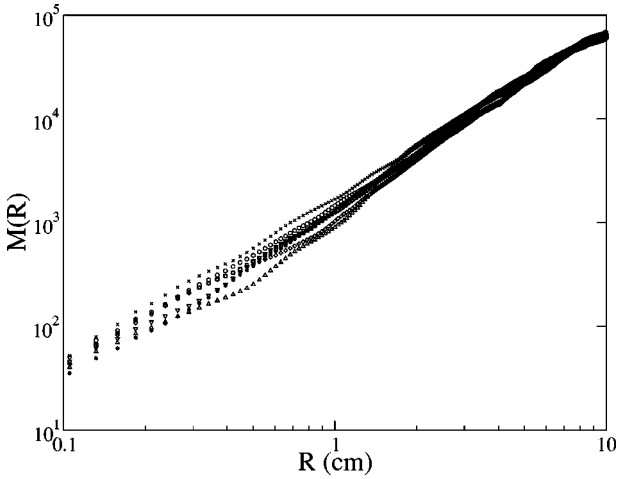

FIG. 3. Mass-size dependence for seven equivalent configurations of CW for (average) $L = 438$ cm. The averaged mass in the scaling region, 0.6 cm $\leqslant R \leqslant 6$ cm, behaves as $M(R) \sim R^D$, $D = 1.9 \pm 0.1$.

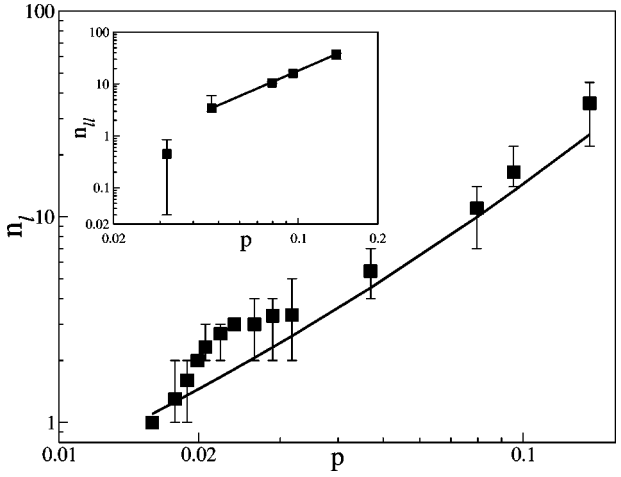

FIG. 4. Log-log plot of the number n_l of loops belonging to a crumpled wire that occupies a fraction p of the area of the cavity as a function of p: (■) experimental data; the continuous line represents the theoretical values obtained from the hierarchical model discussed in the text. The inset shows the number of contacts loop-loop, $n_{ll}(p)$. See text, sixth paragraph.

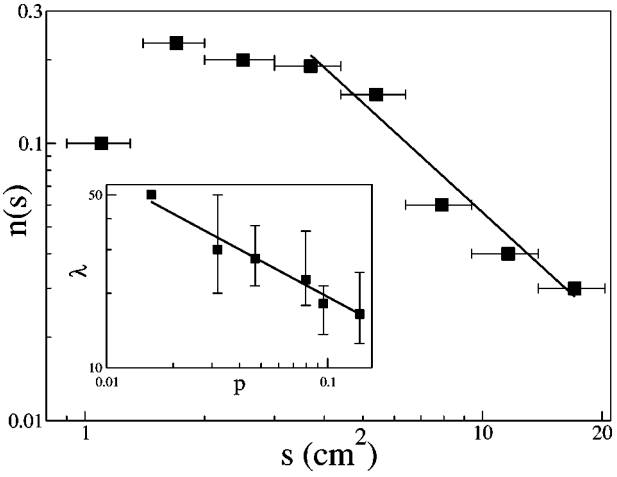

FIG. 5. Experimental (normalized) distribution function $n(s)$ for loops with area s. The straight line indicates the best fit and has a slope of 1.4 ± 0.2 close to the estimate $\tau=1.45\pm0.10$ obtained with the hierarchical model discussed in the text. The inset shows the power-law decay of the average loop size, λ, with p, and the continuous line represents the best fit $\lambda\sim p^{-0.50\pm0.15}$.

are divided in bins according to their respective areas s, we obtain the distribution function $n(s)$, which is shown in Fig. 5. The linear fit in this figure gives an asymptotic power-law behavior over about a decade: $n(s)\sim s^{-1.4\pm0.2}$. The average loop size $\lambda\equiv L/n_l$ decays as $p^{-0.50\pm0.15}$ along one decade of variability in p, as shown in the inset of Fig. 5.

Hierarchical model for CW in 2D. As shown in Fig. 2, loops are the constitutive units of the spatial configurations of CW studied in this Rapid Communication. Let us divide the total number of loops within the cell in a hierarchy of iterations $i=1,2,3,\ldots$ in such a way that at iteration i there are n_i loops with a unitary characteristic perimeter h_i. The total perimeter of all loops is the length L of wire introduced into the cavity, i.e.,

$$L=\sum_{i=1}^{I} n_i h_i, \tag{1}$$

where I is the maximum number of iterations. If we suppose that there are cascades of h_i and n_i controlled, respectively, by two constants η and ν such that $h_{i+1}/h_i=\eta<1$ and $n_{i+1}/n_i=\nu>1$, then we have

$$h_i=\eta^{i-1}h_1, \tag{2a}$$

$$n_i=\nu^{i-1}, \quad i=1,2,\ldots,I, \tag{2b}$$

where h_1 is the perimeter of the largest loop. From the last two equations, we can eliminate i to obtain the distribution function of the perimeter of loops, $n(h)=(h/h_1)^{-D}$, where $D=D(\eta,\nu)=\ln\nu/\ln\eta^{-1}$ is the fractal dimension [10] of the CW in the TP limit (see Fig. 3). If we assume that the area s enclosed by a loop of perimeter h scales as $s\sim h^d$, we find that $n(s)\sim n(h)(dh/ds)\sim h^{-D}s^{(1/d)-1}\sim s^{-(D/d)+(1/d)-1}$, that is,

$$n(s)\sim s^{-\tau}, \quad \tau=\frac{D+d-1}{d}. \tag{3}$$

Using the Euclidean exponent $d=2$, which is valid for the loops in our experiments, and taking $D=1.9\pm0.1$ found in Fig. 3, we get $\tau=1.45\pm0.10$, which is in agreement with the exponent found in Fig. 5. If we adopt the simplest assumption $\nu=2$ in the expression for $D(\eta,\nu)$ above, i.e., if the number of loops duplicates at each iteration, and if we use $D=1.9\pm0.1$, we obtain $\eta=0.69\pm0.01$, which is essentially the experimental value introduced in the fourth paragraph for the ratio $h_1/2\pi R_0$. From now on we will assume that $h_{i+1}/h_i=\eta\equiv\eta_c=0.68$, $\forall i$. Using Eq. (2a), with $\eta=\eta_c$, and Eq. (2b) in Eq. (1) we get

$$L=\frac{L_c[(\eta_c\nu)^I-1]}{[\eta_c\nu-1]}, \tag{4}$$

where $L_c=2\pi R_0\eta_c$, $\eta_c=0.68\pm0.01$, and $\nu=2$.

If we solve Eq. (4) for I and apply the result in the expression for the total number of loops, $n_l=\Sigma\nu_i=(\nu^I-1)/(\nu-1)$, we obtain $n_l=(26.5p+1)^{2.11}-1$ after the substitutions $L=p\pi R_0^2/\zeta$ and $R_0/\zeta=100$. The last expression for $n_l(p)$ is plotted as a solid line in Fig. 4 and shows good agreement with the experimental data. Again from Eq. (4) we obtain $L/L_c\cong2.7[1.3^I-1]$ or $L/R_0\cong11[1.3^I-1]$, and the maximum length of wire which can be introduced into the cavity, $L_{\max}$, depends on the estimate of the maximum number of iterations, $I_{\max}$. An upper bound for $I_{\max}$ is easily obtained if we consider a 2D iterative regular folding process for a wire of length L and width ζ submitted to a shortening ratio of $\frac{1}{2}$ in the length $x_i\equiv(\frac{1}{2})^iL$ and a widening in the transverse direction given by $y_i\equiv2^i\zeta$. This packing process finishes (i.e., a rigid structure is attained) when $i\to I_0$ and

$x_i = y_i$, that is, for $I_0 = \ln(L/\zeta)/\ln 4$. If this upper bound for $I_{\max}$ is introduced in the last equation for L/R_0, we obtain $L_{\max}/R_0 \cong 11[1.3^{\ln(L_{\max}/\zeta)/\ln 4} - 1]$. Numerical solution of this equation for the parameters used in our experiment—$\zeta = 0.1$ cm, $R_0 = 10$ cm—gives $L_{\max,\text{theory}} \cong 420$ cm, which is in good agreement with the average experimental value $\langle L_{\max,\text{exp}} \rangle = 438$ cm. Moreover, we get $I_{\max} < \ln(L_{\max,\text{theory}}/\zeta)/\ln 4 = 6.0$, which means that the theoretic upper bound used for $I_{\max}$ is overestimated by about 13% relative to the average experimental value, $\langle I_{\max,\text{exp}} \rangle \cong 5.2$.

The CW studied in this paper is a disordered 2D cellular structure composed of two different phases, namely air and solid. If $p < 0.14 \pm 0.01$, we can introduce wire in the cavity without difficulty, but as long as the solid fraction p approaches the critical limit 0.14 ± 0.01, the injection of wire in the cavity becomes rapidly difficult and the process of injection is impractical for $p > p_{\max} = 0.14 \pm 0.01$; that is, the crumpled structure becomes rigid.

The authors acknowledge discussions with G. L. Vasconcelos and L. C. de Mélo. This work was supported in part by Conselho Nacional de Desenvolvimento Científico e Tecnológico, Financiadora de Estudos e Projetos, Fundo Setorial do Petróleo, and Programa de Núcleos de Excelência (Brazilian Agencies).

[1] Y. Pomeau, C. R. Acad. Sci., Ser. I: Math. **320**, 975 (1995); M. Ben Amar and Y. Pomeau, Recherche **282**, 45 (1995); I. Perterson, Sci. News (Washington, D.C.) **149**, 376 (1996); G. Gompper, Nature (London) **386**, 439 (1997).

[2] P.A. Houle and J.P. Sethna, Phys. Rev. E **54**, 278 (1996).

[3] A.E. Lobkovsky, S. Gentges, H. Li, D. Morse, and T.A. Witten, Science **270**, 1482 (1995); A.E. Lobkovsky, Phys. Rev. E **53**, 3750 (1996); M. Ben Amar and Y. Pomeau, Proc. R. Soc. London, Ser. A **453**, 729 (1997); E. Cerda and L. Mahadevan, Phys. Rev. Lett. **80**, 2358 (1998).

[4] J.-M. Debierre and R.M. Bradley, J. Phys. A **22**, L213 (1989).

[5] M.A.F. Gomes and V.M. Oliveira, Philos. Mag. Lett. **78**, 325 (1998);

[6] Y. Kantor, M. Kardar, and D.R. Nelson, Phys. Rev. Lett. **57**, 791 (1986); M. Plischke and D. Boal, Phys. Rev. A **38**, 4943 (1988); A. Baumgartner, J. Phys. I **1**, 1549 (1991); F.F. Abraham and M. Kardar, Science **252**, 419 (1991); X. Wen, C.W. Garland, T. Hwa, M. Kardar, E. Kokufuta, Y. Li, M. Orkisz, and T. Tanaka, Nature (London) **355**, 426 (1992); E. Bouchaud and L.-P. Bouchaud, J. Phys. (France) **50**, 829 (1989).

[7] E.M. Kramer and A.E. Lobkovsky, Phys. Rev. E **53**, 1465 (1996).

[8] J.A. Aguiar, M.A.F. Gomes, and A.S. Neto, J. Phys. A **24**, L109 (1991); M.A.F. Gomes, F.F. Lima, and V.M. Oliveira, Philos. Mag. Lett. **64**, 361 (1991); J.B.C. Garcia, M.A.F. Gomes, T.I. Jyh, and T.I. Ren, J. Phys. A **25**, L353 (1992); M.A.F. Gomes and G.S.V. Melo, Philos. Mag. Lett. **68**, 191 (1993).

[9] Digital photographs for all injection geometries are available from the authors upon request.

[10] J. Feder, *Fractals* (Plenum, New York, 1988).

[11] P.-G. de Gennes, *Scaling Concepts in Polymer Physics* (Cornell University Press, Ithaca, NY, 1985).